

The Common Envelope Evolution Outcome. II. Short Orbital Period Hot Subdwarf B Binaries Reveal a Clear Picture

HONGWEI GE ^{1,2,3}, CHRISTOPHER A TOUT ⁴, RONALD F WEBBINK,⁵ XUEFEI CHEN ^{1,2,3}, ARNAB SARKAR ⁴,
JIAO LI ⁶, ZHENWEI LI ^{1,2,3}, LIFU ZHANG ^{1,2,7} AND ZHANWEN HAN ^{1,2,3,7}

¹Yunnan Observatories, Chinese Academy of Sciences,
396 YangFangWang, Guandu District, Kunming, 650216, People's Republic of China
²Key Laboratory for Structure and Evolution of Celestial Objects,
Chinese Academy of Sciences, P.O. Box 110, Kunming 650216, People's Republic of China
³International Centre of Supernovae, Yunnan Key Laboratory,
Kunming 650216, People's Republic of China
⁴Institute of Astronomy, The Observatories, University of Cambridge,
Madingley Road, Cambridge, CB3 0HA, UK
⁵University of Illinois at Urbana-Champaign, 1002 W Green St, Urbana, 61801, USA
⁶Key Lab of Space Astronomy and Technology, National Astronomical Observatories,
Chinese Academy of Sciences, Beijing 100101, People's Republic of China
⁷University of Chinese Academy of Sciences, Beijing 100049, People's Republic of China

ABSTRACT

Common envelope evolution (CEE) is vital to form short orbital period compact binaries. It covers many objects, such as double compact merging binaries, type Ia supernovae progenitors, binary pulsars and X-ray binaries. Knowledge of the common envelope (CE) ejection efficiency still needs to be improved, though progress has been made recently. Short orbital period hot subdwarf B star (sdB) plus white dwarf (WD) binaries are the most straightforward samples with which to constrain CEE physics. We apply the known orbital period–white dwarf mass relation to constrain the sdB progenitors of seven sdB+WD binaries with a known inclination angle. The average CE efficiency parameter is 0.32. This is consistent with previous studies. However, the CE efficiency need not be constant but a function of the initial mass ratio based on well-constrained sdB progenitor mass and evolutionary stage. Our results can be used as physical inputs for binary population synthesis simulations of related objects. A similar method can also be applied to study other short orbital period WD binaries.

Keywords: Binary Stars(154) — B subdwarf Stars(129) — Stellar Physics(1621) — Common Envelope Evolution(2154)

1. INTRODUCTION

The common envelope (CE) phase is fundamental to binary star evolution. The common envelope evolution

(CEE) is vital in the formation of short orbital period binaries of one or two compact objects (Livio & Soker 1988; Taam & Sandquist 2000; Ivanova et al. 2013). These systems cover a broad range of progenitor masses and types, such as merging black-hole–black-hole, black-hole–neutron-star, and neutron-star–neutron-star binaries (e.g., Broekgaarden et al. 2021; Olejak et al. 2021; Shao & Li 2021; Gallegos-Garcia et al. 2023; Iorio et al. 2023), type Ibn/Icn supernovae from merging Wolf-Rayet/black hole (Metzger 2022), type IIb supernovae (Soker 2017), luminous red novae (e.g., Matsumoto &

gehwh@ynao.ac.cn

cat@ast.cam.ac.uk

rwebbink@illinois.edu

zhanwenhan@ynao.ac.cn

Metzger 2022; Cai et al. 2022), type Ia supernovae progenitors (e.g., Wang 2018; Kashi & Soker 2011), binary pulsars (e.g., Chen & Liu 2013; Liu et al. 2018), X-ray binaries (e.g., Tauris et al. 2000; Podsiadlowski & Rappaport 2000), double white dwarfs (e.g., Li et al. 2023), cataclysmic variables (e.g., Webbink 1984), and planetary nebulae with binary nuclei (e.g., Livio & Soker 1988). For a comprehensive review, we refer the reader to Ivanova et al. (2013), Röpke & De Marco (2023) or Tauris & van den Heuvel (2023).

A standard method to constrain the CEE outcome is the energy formalism (Webbink 1984; Iben & Tutukov 1984; Livio & Soker 1988). However, the quantitative parameters in binary mass-transfer physics, such as CE efficiency α_{CE} remain poorly studied. For example, the merging rate of double neutron stars can vary by two orders of magnitude for different CE efficiency (Belczynski et al. 2002). We can use different types of observed post-CE binaries to constrain the CEE physics. Benefiting from the well-known formation channel of short orbital-period hot subdwarf binaries, we use these objects to constrain the CEE outcome.

Hot subdwarf stars of spectral types B and O (sdB/Os) are located around the bluest end of the horizontal branch and roughly between the main sequence (MS) and white dwarf (WD) sequence in the Hertzsprung–Russell diagram (reviewed by Heber 2009, 2016). Their surface temperatures and surface gravities are relatively high, i.e., $20,000 \text{ K} \leq T_{\text{eff}} \leq 70,000 \text{ K}$ and $5.0 \leq \log_{10} (\text{g}/\text{cm s}^{-2}) \leq 6.5$ (Heber 2016; Lei et al. 2023). Based on a catalogue of 39,800 hot subluminescent star candidates, over one thousand sdB/Os have been identified with the Large Sky Area Multi-Object Fiber Spectroscopic Telescope spectra (Luo et al. 2021; Lei et al. 2023). Geier (2020) compiled an updated catalogue of 5874 hot subdwarf stars. Most of the sdBs are core helium-burning stars of about $0.5 M_{\odot}$, with a thin envelope, on the extreme horizontal branch. About half of the sdBs reside in close binary systems (Maxted et al. 2001; Copperwheat et al. 2011). About one-third of sdB binaries have a MS companion with a long orbital period of a few hundred days (Vos et al. 2018). In addition, about two-thirds of sdB binaries have a WD, a typical M-type low-mass MS star or a brown dwarf (BD) companion with short orbital periods from about 1 hr to 30 d (Kupfer et al. 2015; Schaffenroth et al. 2022, 2023).

Short orbital period sdB binaries with WD companions can constrain the CE efficiency because they likely form after a first stable mass transfer phase and a second unstable CE phase (Han et al. 2003; Podsiadlowski et al. 2008). After the first mass transfer phase, there is a well-known orbital period–WD mass ($P_{\text{orb}}-M_{\text{WD}}$)

relation (Refsdal & Weigert 1971). Hence, the sdB progenitor mass and evolutionary stage can be well determined through the WD mass in an observed sdB+WD system. We calculate the binding energy by tracing the precise change of donor’s total energy as a function of its remnant mass (Ge et al. 2010a, 2022).

Section 2 introduces the formation channel of short orbital period sdBs with WD companions and the $P_{\text{orb}}-M_{\text{WD}}$ relation. Section 3 describes our method to calculate the binding energy and determine the CE efficiency parameter by constraining the sdB progenitor’s mass and evolutionary stages. We present our results of the CE efficiency from the energy and angular momentum descriptions in Section 4. We discuss the uncertainties and make a comparison with previous studies in Section 5, 6 and 7. Section 8 summarizes and concludes our knowledge of CEE from short orbital period sdB+WD binaries.

2. HOT SUBDWARF B STAR WITH A WHITE DWARF COMPANION

Radial velocity surveys of sdBs have provided orbital parameters of such binary systems (e.g., Maxted et al. 2001; Geier et al. 2011; Copperwheat et al. 2011). With this benefit, the number of short-period sdB binaries with known orbits has increased rapidly to over 140 (Kupfer et al. 2015; Kawka et al. 2015). Also, Schaffenroth et al. (2022, 2023) derive the nature of the primaries and secondaries of more sdB binaries by classifying the space-based light-curve variations and combining these with a fit to the spectral energy distribution, the distance derived from Gaia, and the atmospheric parameters. Among these short orbital period sdB binaries (Kupfer et al. 2015; Schaffenroth et al. 2023) over half contain a WD companion. At the same time about a quarter are accompanied by a MS/BD star. For the rest, the type of the sdB’s companions is still undecided between a MS/BD or a WD.

To precisely constrain the CE evolution physics, we need to have accurate masses of the sdB and its companion. The masses of two companions can be derived from the well-known binary mass function,

$$f_m = \frac{M_{\text{comp}}^3 \sin^3 i}{(M_{\text{comp}} + M_{\text{sdB}})^2} = \frac{P_{\text{orb}} K_1^3}{2\pi G}, \quad (1)$$

where P_{orb} is the orbital period and K_1 is the amplitude of the radial velocity variation. The sdB mass M_{sdB} and the companion mass M_{comp} are found when the inclination angle i is known. Typically, we expect orbital inclinations to the line of sight to be uniformly distributed over a sphere. So, the distribution of $\cos i$ is flat. The minimum mass for the companion can be determined if

we assume an inclination $i = \pi/2$. For a large sample of sdB binaries, we can research the inclination angle distribution and statistical features. However, we focus on precisely constraining the CE ejection process. So, we analyze short orbital sdB binaries with known inclinations (see Figure 1 and Table 1 with data partially from Schaffenroth et al. 2023). The orbital parameters (period P_{orb} , system velocity Γ , radial velocity semi-amplitude K_1 , inclination angle i , and separation A) as well as the WD mass M_{WD} , sdB mass M_{sdB} , effective temperature T_{eff} and surface gravity $\log g$ are listed in Table 1.

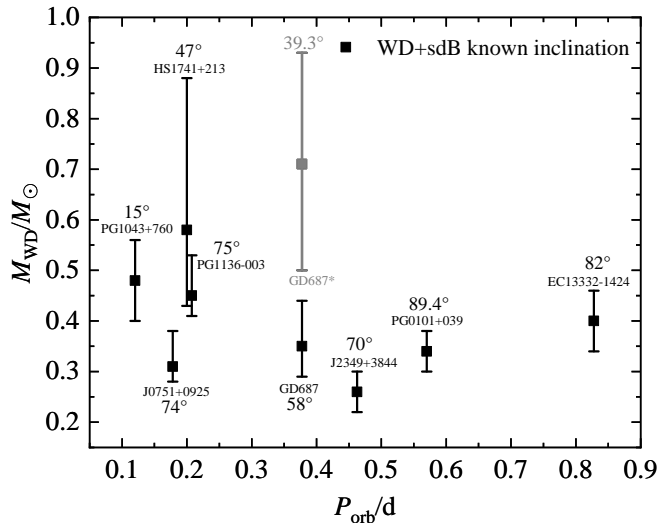


Figure 1. The observed orbital periods and white dwarf masses of 8 hot subdwarf B and white dwarf binaries with known inclination angles (Schaffenroth et al. 2023). The gray line marks the observed data of Geier et al. (2010).

Unlike the short orbital sdB + MS binaries, most short orbital sdB + WD binaries can help us narrow down the progenitor mass of a sdB with the benefits from their first mass-transfer process. Consequently, observed short orbital sdB + WD binaries help us constrain the CE physics more precisely.

2.1. First Stable Mass Transfer Matters

Heber (2016) reviewed the formation channels of sdB binaries in detail. The three main scenarios were proposed more than forty years ago. These are the CE evolution (Paczynski 1976), stable mass transfer (also known as Roche-lobe overflow), and merging WDs (Webbink 1984). Isolated sdB stars might be formed by the merging of two helium WDs (Saio & Jeffery 2000; Zhang & Jeffery 2012) or that of a red-giant core with

a low-mass star, a brown dwarf or a planet (Soker 1998; Politano et al. 2008). Long orbital period sdB binaries, from 10 to over 1000 d, are likely formed when a red-giant donor loses its envelope through dynamically stable mass transfer to a MS companion (Han et al. 2003; Podsiadlowski et al. 2008; Chen et al. 2013). Short orbital period sdB binaries, from about 1 hr to 30 d, undergo at least one CE phase in principle. If the companion is a MS star, the sdB binary suffers only one CE evolution.

On the other hand, a short orbital sdB binary with a WD companion is likely formed after a first stable mass transfer phase and a second unstable CE phase (Han et al. 2003; Podsiadlowski et al. 2008). Notably, a critical mass ratio for instability $q_{\text{crit}} \equiv M_{\text{donor}}/M_{\text{accretor}} = 1.2$ or 1.5 is typically adopted, independent of the progenitor mass of an sdB. Recent studies by Ge et al. (2020a, 2023, 2020b) show that the critical mass ratios for dynamically unstable q_{ad} or thermal timescale mass transfer q_{th} depend on both the progenitor mass and evolutionary stage (the radius).

We need to know the progenitor mass, initial mass ratio, and initial period before the CE as well as the final remnant mass, final mass ratio and final orbital period after the CE to fit the CE evolution precisely (right panel of Figure 2). For short orbital period sdB binaries with WD companions, the current masses of both companions and orbital period or separation after the second CE evolution are known. The progenitor mass of sdB before the second CE evolution can be constrained by considering the first stable mass transfer phase (left panel of Figure 2). After this phase, the $P_{\text{orb}}-M_{\text{WD}}$ relation means the WD and progenitor mass do not pair arbitrarily. Because the progenitors of sdBs are almost all located at the tip of the red giant branch (TRGB), where radii are a function of mass.

2.2. Period–White Dwarf Mass Relation

Refsdal & Weigert (1971) found a relation between helium WD mass M_{WD} and orbital separation A through slow and conservative Case B (Kippenhahn & Weigert 1967) mass transfer for a set of $2.5M_{\odot}$ total-mass binaries. The first reason comes from the well-known core mass–radius ($M_{\text{c}}-R$) relation for giants (Paczynski 1971a; Webbink et al. 1983; Joss et al. 1987). This $M_{\text{c}}-R$ relation derives from the luminosity L depending only on the core mass M_{c} and the radius R depending only on the luminosity L and total mass M_{d} for donor stars with degenerate cores. We illustrate the core mass M_{c} and inner core mass of $Z = 0.02$ donor stars on the mass and radius diagram in Figure 3. Stellar model grids in this figure are collected from detailed numerical simu-

Table 1. Observed short orbital period sdB binaries with a white-dwarf companion

Name1	P_{orb}/d	$\Gamma/\text{km s}^{-1}$	$K_1/\text{km s}^{-1}$	i	A/R_{\odot}	M_{WD}/M_{\odot}	M_{sdB}/M_{\odot}	T_{eff}/K	$\log_{10}(\text{g/cm s}^{-2})$
PG1043+760	0.12015	24.8	63.6	15.0 ± 0.6	0.94 ± 0.04	$0.48^{+0.08}_{-0.08}$	0.291	27600 ± 800	5.39 ± 0.10
GALEXJ075147.0+092526	0.17832	15.5	147.7	74.0 ± 10.0	1.19 ± 0.08	$0.31^{+0.07}_{-0.03}$	0.365	30620 ± 490	5.74 ± 0.12
HS1741+213	0.20000	...	157.0	47.0 ± 11.0	1.40 ± 0.30	$0.58^{+0.30}_{-0.15}$	0.400	35600	5.30
PG1136-003	0.20754	23.3	162.0	75.0 ± 11.0	1.40 ± 0.10	$0.45^{+0.08}_{-0.04}$	0.501	31200 ± 600	5.54 ± 0.09
GD687	0.37765	32.3	118.3	58.0 ± 8.0	1.90 ± 0.20	$0.35^{+0.09}_{-0.06}$	0.283	24300 ± 500	5.32 ± 0.07
GD687*	0.37765	32.3	118.3	39.3 ± 6.0	2.32 ± 0.20	$0.71^{+0.22}_{-0.21}$	0.470	24300 ± 500	5.32 ± 0.07
GALEXJ234947.7+384440	0.46252	2.0	87.9	70.0 ± 10.0	2.20 ± 0.20	$0.26^{+0.04}_{-0.04}$	0.406	28400 ± 00	5.40 ± 0.30
PG0101+039	0.56990	7.3	104.7	89.4 ± 0.6	2.53 ± 0.01	$0.34^{+0.04}_{-0.04}$	0.416	32200	5.79
EC13332-1424	0.82794	-53.2	104.1	82.0 ± 2.0	3.40 ± 0.20	$0.40^{+0.06}_{-0.06}$	0.400

NOTE—Objects and data are mostly from partial results of Schaffenroth et al. (2023, and references therein) while * marks that of Geier et al. (2010).

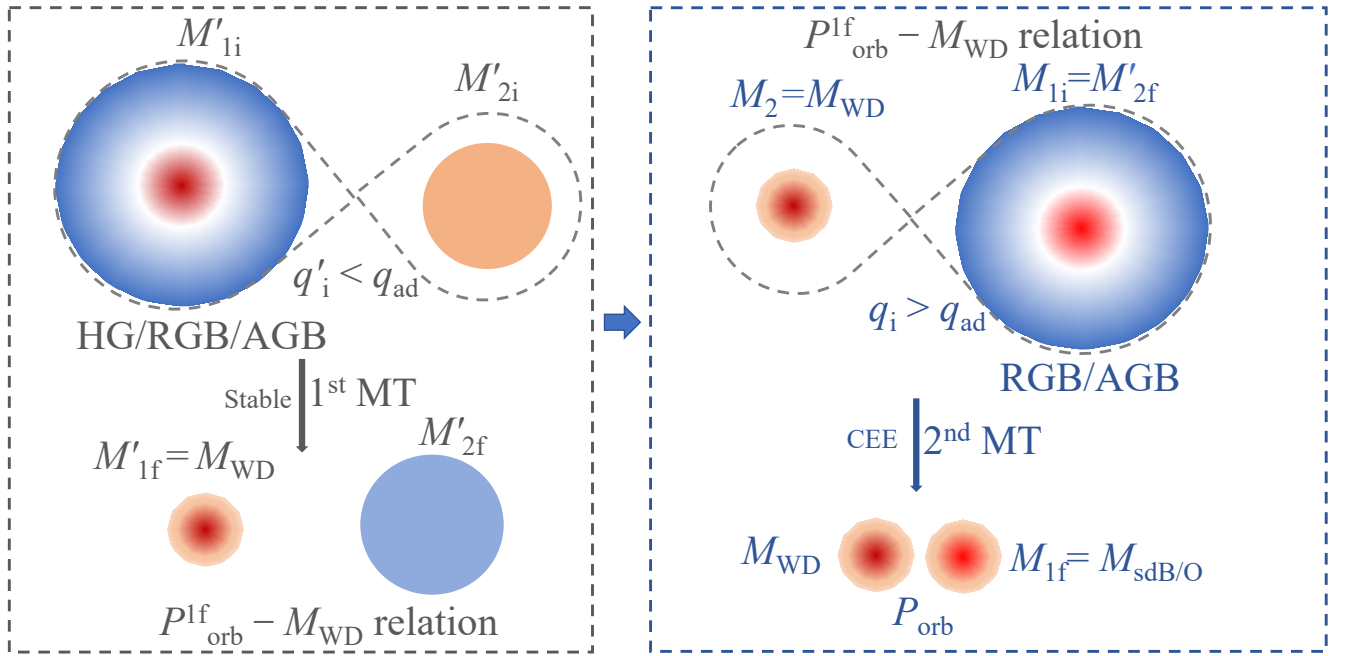


Figure 2. A typical formation channel for a close hot subdwarf B/O star (sdB/O) plus white dwarf (WD) binary. The orbital period and WD mass relation after the first stable mass transfer process consequently impact the pairing of the WD mass and the secondary mass M_2 . This is because the secondary radius around the tip of the red giant branch is a function of its mass M_2 (see the second solid line from top in Figure 3). The period-white dwarf mass relation is consistent to some degree with the distribution of the progenitors of sdB binaries before the second Common Envelope (CE) phase in the separation–secondary mass plane (figure 7 of Han et al. 2003).

lations by (Ge et al. 2020a). The second reason stems from mass-transfer physics. The Roche-lobe radius of the donor star, for mass ratio $0 < M_d/M_a < 0.8$, can be approximated by

$$R_L = \frac{2}{3^{4/3}} A \left(\frac{M_d}{M_d + M_a} \right)^{1/3} \quad (2)$$

(Paczynski 1971b), where M_a is the mass of the accretor. From Kepler’s law, we have

$$\left(\frac{2\pi}{P_{\text{orb}}} \right)^2 A^3 = G (M_d + M_a), \quad (3)$$

where P_{orb} is the orbital period and G is Newton's gravitational constant. For a binary system undergoing stable mass transfer (Roche-lobe overflow, RLOF), the donor radius R almost closely tracks its Roche-lobe radius R_L . Combining the above knowledge from mass transfer physics, we find that the total mass of the donor and accretor is eliminated. Rappaport et al. (1995) derived the expression for the orbital period

$$P_{\text{orb}} = 20 G^{-1/2} R^{3/2} M_d^{-1/2}. \quad (4)$$

The core mass–radius relation can be used in Equation (4), and the remnant mass M_{WD} of a donor with a degenerate core is close to the core mass M_c . So, after stable mass transfer stops, we expect a relation between the orbital period P_{orb} and the donor's remnant mass M_{WD} .

Rappaport et al. (1995, hereinafter RPJDH95) studied the detailed mass transfer process in a binary system, initially containing a neutron star and a low-mass giant and finally ending up as a wide binary comprising a radio pulsar and a WD (see, e.g., Bhattacharya & van den Heuvel 1991). RPJDH95 devised a fitting formulae for $P_{\text{orb}}-M_{\text{WD}}$ relations,

$$\frac{P_{\text{orb}}}{\text{d}} = 0.374 \left[\frac{\left(\frac{R_0}{R_\odot}\right) \left(\frac{M_{\text{WD}}}{M_\odot}\right)^{4.5}}{\left(1 + 4 \left(\frac{M_{\text{WD}}}{M_\odot}\right)^4\right)} + 0.5 \right]^{3/2} \left(\frac{M_{\text{WD}}}{M_\odot}\right)^{-1/2}. \quad (5)$$

The above relations cover core mass range $0.15 < M_{\text{WD}}/M_\odot < 1.15$. The radii R_0 depend on the metallicity Z . For $Z = 0.02$ stellar models, $Z = 0.001$ models, and all combined models, R_0 equals $5500 R_\odot$, $3300 R_\odot$, and $4950 R_\odot$, respectively.

Using an updated Cambridge STARS code (Pols et al. 1995), Tauris & Savonije (1999, hereinafter TS99) derived new $P_{\text{orb}}-M_{\text{WD}}$ correlations based on 121 LMXB models. The best fit for all models is

$$\frac{M_{\text{WD}}}{M_\odot} = \left(\frac{(P_{\text{orb}}/\text{d})}{b}\right)^{1/a} + c, \quad (6)$$

where, depending on the chemical composition of the donor,

$$(a, b, c) = \begin{cases} (4.50, 1.2 \times 10^5, 0.120) & Z = 0.02 \\ (4.75, 1.1 \times 10^5, 0.115) & \text{Combined} \\ (5.00, 1.0 \times 10^5, 0.110) & Z = 0.001. \end{cases} \quad (7)$$

Chen et al. (2013, hereinafter CHDP13) presented a systematic study (extended by Zhang et al. 2021a) of the long-period sdB binaries. They found that sdB binaries produced from stable mass transfer follow a unique $P_{\text{orb}}-M_{\text{WD}}$ relation for progenitor masses below the helium

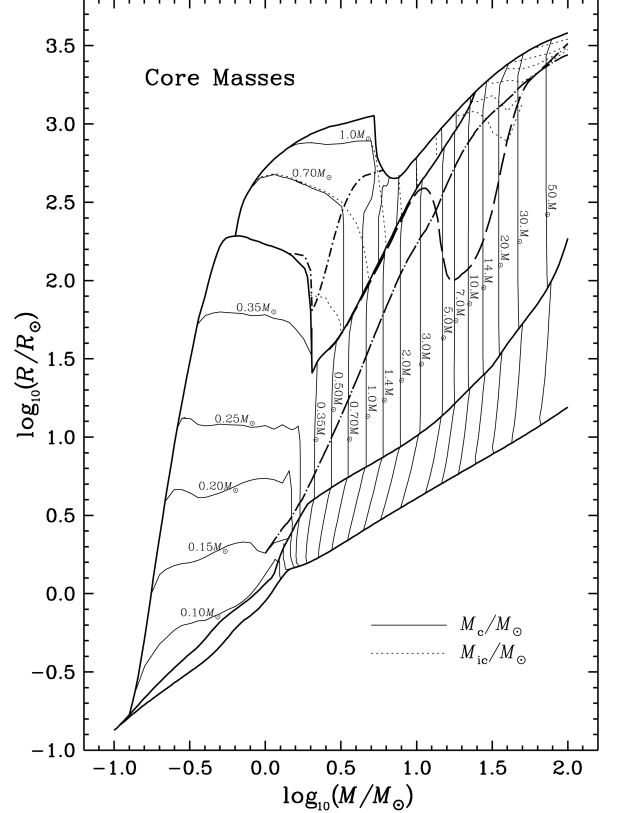


Figure 3. Core masses M_c and inner core masses M_{ic} on the mass–radius diagram. Stellar models cover a mass range from 0.1 to $100 M_\odot$ with metallicity $Z = 0.02$ (Ge et al. 2020a). The thick solid lines mark crucial evolutionary stages, the zero-age main sequence (ZAMS), the terminal main sequence (TMS), the tip of the red giant branch (BGB) and the tip of the asymptotic giant branch (TAGB). The dash-dotted line labels the base of red giant branch (BGB). The thin-solid and thin-dotted lines show all stars' core and inner core masses at different evolutionary stages. The masses, M_c and M_{ic} mark the midpoints in hydrogen and helium depletion profiles, respectively. In other words, the core mass M_c refers to the mass coordinate at which the helium abundance is halfway between the surface helium abundance and the maximum helium abundance in the stellar interior. The inner core mass M_{ic} identifies the mass coordinate at which the helium abundance is halfway between the maximum helium abundance in the stellar interior and the minimum helium abundance interior to that maximum.

flash limits. The remnant mass in this study covers a relatively massive range from 0.37 to $0.51 M_\odot$. Smedley et al. (2014) examined binary millisecond pulsars that form after a stable mass transfer phase from a low to intermediate mass companion, between central hydrogen exhaustion and core helium ignition, to a neutron star. They confirmed that their stellar models reproduced a

well-defined $P_{\text{orb}}-M_{\text{WD}}$ relation,

$$\frac{P_{\text{orb}}}{\text{d}} = \exp \left(a + \left(\frac{b}{M_{\text{WD}}/M_{\odot}} \right) + c \left(\ln \frac{M_{\text{WD}}}{M_{\odot}} \right) \right), \quad (8)$$

with

$$(a, b, c) = \begin{cases} (22.902, 3.097, 23.483) & 0.170 \leq M_{\text{WD}} < 0.225 \\ (14.443, 0.335, 9.481) & 0.225 \leq M_{\text{WD}} < 0.280 \\ (11.842, -3.831, -4.146) & 0.280 \leq M_{\text{WD}} < 0.480. \end{cases} \quad (9)$$

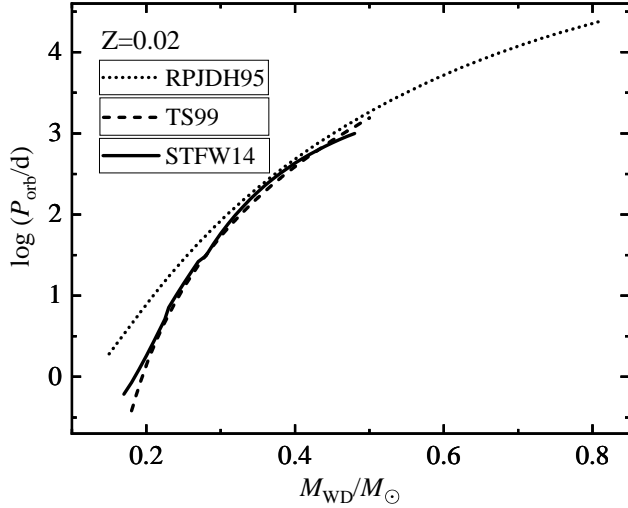


Figure 4. The period–WD mass ($P_{\text{orb}}-M_{\text{WD}}$) relation shows in the works of literature (metallicity $Z = 0.02$). The dotted line, dashed line, and solid line represent the fitting formulae by Rappaport et al. (1995, RPJDH95), Tauris & Savonije (1999, TS99), and Smedley et al. (2014, STFW14), respectively. We cut the WD mass off at around $0.8 M_{\odot}$ because of the upper limit of the minimum WD masses (Schafneroth et al. 2022).

The $P_{\text{orb}}-M_{\text{WD}}$ relations from different studies share a similar slope. However, the $P_{\text{orb}}-M_{\text{WD}}$ relation difference becomes significant for relatively less massive ($M_{\text{WD}} < 0.35 M_{\odot}$) WDs (see Figure 4). For Pop II stars ($Z = 0.001$), the orbital period is systematically smaller than that for $Z = 0.02$ stars with the same WD mass (RPJDH95, TS99, and STFW14). Different chemical abundances and mixing length parameters can change the orbital period in the $P_{\text{orb}}-M_{\text{WD}}$ relation by a factor of 2.4 (RPJDH95). It should be noticed first that the orbital period is independent of the accretor mass (all previous studies and Equation 4). Furthermore the $P_{\text{orb}}-M_{\text{WD}}$ relation is not much affected by the non-conservative nature of stable mass transfer (TS99, CHDP13, and STFW14) and so the fraction of mass or

angular momentum loss from the binary system. However, for an individual binary, TS99 pointed out that P_{orb} and M_{WD} increase with increasing fractions of mass and angular momentum loss. Gao & Li (2023) studied the $P_{\text{orb}}-M_{\text{WD}}$ relation under wind mass-loss and pointed out that tidally enhanced wind can play an important role for helium WD binaries in wide orbits. In addition, the $P_{\text{orb}}-M_{\text{WD}}$ relation is ascertained from a circular orbit. For some binary pulsars with a possible neutron star or massive WD ($M > 0.8 M_{\odot}$), the eccentricity is high ($e > 0.025$, see RPJDH95). Such high eccentricity is not the case for progenitors of sdB+WD binaries and it is safe to assume a circular orbit in this study. Finally, in this study, we mainly focus on low-mass donors with $M_{\text{d}} < 2.0 M_{\odot}$ and so the P_{orb} and M_{WD} relation fits well for these stars. However, there is a slight deviation of the P_{orb} and M_{WD} relation for more massive donors (see TS99 and Figure 7 of Han et al. 2003). TS99 explained this because the mass transfer becomes dynamically unstable for $M_{\text{d}} > 2.0 M_{\odot}$ stars. A systematical study of the criteria for dynamical timescale mass transfer by Ge et al. (2020a) shows that $6.3 M_{\odot} > M_{\text{d}} > 1.8 M_{\odot}$ giant stars more easily enter dynamically unstable mass transfer than less massive giants (see Figures 6 and 7 of Ge et al. 2020a).

3. METHODS

We study the CE ejection process under the assumption that it is adiabatic. This might not be entirely appropriate for the whole ejection process. However, it works to constrain the initial and final state of CE evolution. After the hydrodynamical interaction, the remnant star could relax to hydrostatic and subsequent thermal equilibrium. The adiabatic mass loss model and the code have been introduced in detail by Ge et al. (2022, hereinafter Paper I). The physical inputs and control parameters, such as opacity tables and the mixing length parameter, are described in Paper I and references therein.

We follow a standard procedure to predict the outcome of CE evolution. This is based on the essential physics of total energy conservation, known as the energy formalism (Webbink 1984; Iben & Tutukov 1984; Livio & Soker 1988). It is written as

$$\alpha_{\text{CE}} \Delta E_{\text{orb}} = E_{\text{bind}}, \quad (10)$$

where α_{CE} is the CE efficiency parameter, the fraction of the orbital energy change ΔE_{orb} used to overcome the envelope’s binding energy E_{bind} .

After a dimensionless parameter λ is introduced in the binding energy term, the formula is often written as

(Webbink 1984; de Kool 1990)

$$\alpha_{\text{CE}} \left(\frac{GM_{1i}M_2}{2A_i} - \frac{GM_{1f}M_2}{2A_f} \right) = -\frac{GM_{1i}M_{1e}}{\lambda R_{1i}}, \quad (11)$$

where G is Newton's gravitational constant, M_{1i} and M_{1f} are the initial and final mass of the donor, M_2 is the accretor's mass assumed not to change, A_i and A_f are the initial and final semimajor axes, $M_{1e} = M_{1i} - M_{1f}$ is the envelope mass of the donor, R_{1i} is the initial radius of the donor and λ is a dimensionless parameter that reflects the structure of the donor star. This λ was previously assumed to be 0.5 in binary population synthesis studies. However, many recent works (Tauris & Dewi 2001; Xu & Li 2010; Loveridge et al. 2011; De Marco et al. 2011) aimed precisely calculate it and significantly improved our knowledge of the binding energy of stars with different masses and evolutionary stages.

The binding energy can be calculated for the initial giant as

$$\begin{aligned} E'_{\text{bind}} &= \int_{M_c}^{M_{1i}} \left(-\frac{Gm}{r} + \alpha_{\text{th}}U \right) dm, \\ &= E_{\text{grav}} + \alpha_{\text{th}}E_{\text{th}} \end{aligned} \quad (12)$$

where α_{th} is defined as the fractional contribution of the internal energy (Han et al. 1995) or thermal efficiency. We assume $\alpha_{\text{th}} = 1$ throughout this paper unless specific notes are made. The core response, after the CE ejection, is neglected in this expression. This is fine for donor stars with degenerate cores. However, it can cause problems for massive stars with non-degenerate cores. In particular, companions of massive stars with different masses could spiral into different depths inside the non-degenerate core. As described in Paper I, we calculate the binding energy E_{bind} by tracing the change of the total energy of the donor as the mass is lost (Ge et al. 2010a),

$$\begin{aligned} \Delta E_1 \equiv -E_{\text{bind}} &= \int_0^{M_{1f}} \left(-\frac{Gm}{r} + U \right) dm \\ &\quad - \int_0^{M_{1i}} \left(-\frac{Gm}{r} + U \right) dm, \end{aligned} \quad (13)$$

where m is the donor mass, r is the radius and U is its specific internal energy including recombination part. The final mass M_{1f} is not fixed to the core mass M_c as usual but determined by when the remnant first shrinks back inside its Roche lobe $R_{1f} < R_{1,L1}$. Our method considers the redistribution of the remnant core with a thin envelope and the impact of the companion mass. In addition, we also compare the companion's radius R_2 to its Roche lobe radius $R_{2,L1}$. So, we have

$$R_{1f} \leq R_{1,L1}, \text{ and } R_2 \leq R_{2,L1}, \quad (14)$$

for a successive CE ejection. If $R_{1f} \leq R_{1,L1}$ and $R_2 \leq R_{2,L1}$, the envelope is, in principle, ejectable. Otherwise, the CE evolution ends with merging if $R_{1f} > R_{1,L1}$ and $R_2 > R_{2,L1}$. Aside from the role of the donor, the companion type could play an important role in the outcome of CE evolution. The MS companion radius may be larger than its Roche-lobe radius if its mass is too close to the donor mass. So, a non-compact companion with mass close to its donor may cause the stars to merge in CE evolution. However, the WD companion radius is almost always smaller than its Roche-lobe radius.

3.1. The Initial to Final Separation Relation in Different Formalisms

With the calculation of binding energy in Equation 13, we define the CE efficiency parameter as β_{CE} to distinguish from the binding energy calculation in Equation 11. The final to initial separation relation can be written as

$$\frac{A_f}{A_i} = \frac{M_{1f}}{M_{1i}} \left(1 + \frac{2A_i \Delta E_1}{\beta_{\text{CE}} G M_2 M_{1i}} \right)^{-1}. \quad (15)$$

We apply our constraint to CE evolution using short orbital period sdB plus WD binaries and present our results in the next section. We compare our results to recent studies by Hernandez et al. (2022), Zorotovic & Schreiber (2022) and Scherbak & Fuller (2023) on WD binaries with low-mass main-sequence, white dwarf companions or brown dwarf companions. So, we introduce here other formulae that predict the outcome of CE evolution from its initial conditions that differ from the energy conservation description.

Di Stefano et al. (2023) use angular momentum in a new way to derive a simple expression for the final orbital separation and their method is well suited to higher-order multiples. We adopt their expressions for the η formalism (Di Stefano et al. 2023), the γ formalism (Nelemans et al. 2000; Nelemans & Tout 2005), and the α formalism (Webbink 1984; de Kool 1990). The η formalism is written as

$$\begin{aligned} \frac{A_f}{A_i} &= \left[\frac{(1+q)(1+q_{\text{ec}})^2}{1+q(1+q_{\text{ec}})} \right] \\ &\quad \times \exp \left[-2\eta \left(\frac{q q_{\text{ec}}}{1+q} \right) \mathcal{F}(q, \delta) \right], \end{aligned} \quad (16)$$

where

$$\mathcal{F}(q, \delta) = \mathcal{Q}(q, \delta) \frac{1}{q} + \mathcal{Q} \left(\frac{1}{q}, \delta \right) q, \quad (17)$$

and

$$\mathcal{Q}(q, \delta) \equiv \frac{[f(q)]^\delta}{[f(q)]^\delta + [f(q^{-1})]^\delta}. \quad (18)$$

The function of $f(q)$ is defined by Eggleton (1983) as

$$f(q) = r_L(q) = \frac{R_L}{A} = \frac{0.49q^{\frac{2}{3}}}{0.6q^{\frac{2}{3}} + \ln\left(1 + q^{\frac{1}{3}}\right)}, \quad (19)$$

and the mass ratios $q \equiv M_{1f}/M_2$ while $q_{ec} \equiv M_{1e}/M_{1f}$. They suggest using $\delta = 3$ to constrain the post-CE binaries. The α formalism can be rewritten as

$$\frac{A_i}{A_f} = (1 + q_{ec}) \left(1 + \frac{2q_{ec}q}{\alpha_{CE}\lambda} [f(q + q_{ec}q)]^{-1}\right), \quad (20)$$

and the γ formalism for

$$\frac{A_i}{A_f} = \left[\frac{1}{1 + q_{ec}}\right]^2 \left[\frac{1 + q(1 + q_{ec})}{1 + q}\right] \times \left[\frac{1 + q(1 + q_{ec})}{1 + q + q_{ec}(1 - \gamma)}\right]^2. \quad (21)$$

3.2. The Model Grids for the Progenitors of Hot Subdwarf B Stars

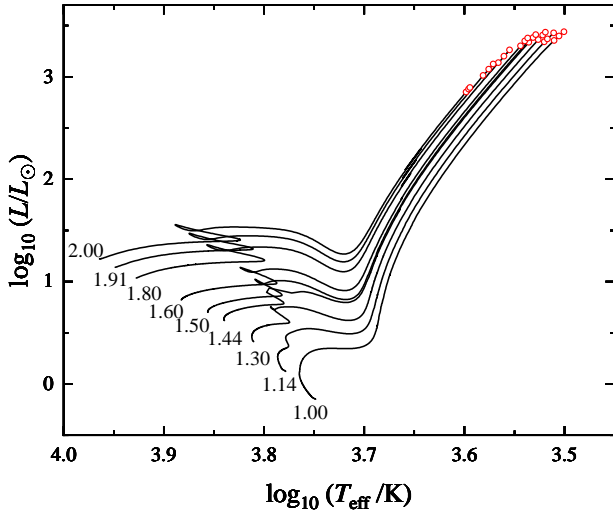


Figure 5. Model grids for sdB progenitors are marked with red open circles. The evolutionary stages in a narrow region near the TRGB with masses from 1.00 to 2.00 M_\odot and metallicity $Z = 0.02$.

In Paper I, we aim to preliminarily check the precisely calculated binding energy of which the response of the donor remnant and the effects of companion mass are naturally considered. However, the progenitor masses of the observed sdBs are not strictly constrained. We apply the $P_{orb}-M_{WD}$ relation to constrain the progenitor mass for sdB+WD binaries. The progenitor model grids are extended as shown in Figure 5. The mass grids are expanded to 1.00, 1.14, 1.30, 1.44, 1.50, 1.60, 1.80, 1.91, and 2.00 M_\odot . The evolutionary stages are covered

in a narrow region (Han et al. 2002; Zhang et al. 2021b) near the TRGB (open circles in Figure 5). We ignore progenitors with a mass larger than 2 M_\odot because the $P_{orb}-M_{WD}$ relation is likely unsuitable for RGB stars with non-degenerate cores. The influence of this should be negligible in our study because most of the progenitor masses of sdBs are likely around 1.0 to 1.3 M_\odot .

With the model grids, we trace the radius response and the total energy change (Equation 13) of the donor using the adiabatic mass-loss code (Ge et al. 2010a,b, 2015, 2020a, 2023). We first assume the progenitor masses of eight sdB binaries with a WD companion in Table 1 are 1.00, 1.14, 1.30, 1.44, 1.50, 1.60, 1.80, 1.91, and 2.00 M_\odot . Starting with an initial guess of $\beta_{CE} = 0.5$ we use a bisection method to solve Equations 13, 14, 15 and 1. According to the difference between the derived orbital period and observed orbital period, we adjust the theoretical CE efficiency parameter. Then, we solve for the CE efficiency parameter β_{CE} that satisfies the sdB mass M_{sdB} , the WD companion mass M_{WD} , the inclination angle i , the amplitude K_1 , and the orbital period P_{orb} . Secondly we constrain the β_{CE} range using the error bar of the observed WD mass.

Finally, we restrict the possible β_{CE} by determining the progenitor mass of sdB via the $P_{orb}-M_{WD}$ relation. With known M_{WD} in an sdB + WD binary, the theoretical orbital period P_{theo} is calculated by Equation 8 from STF14. The initial separation A_i just before the CE can also be determined from the Roche-lobe radius of the donor

$$A_i = \frac{R_L}{r_L(q)} = \frac{R_{li}}{r_L(M_{1i}/M_2)}. \quad (22)$$

The initial orbital period P_i can be derived from Kepler's third Law.

4. RESULTS

We first assume the progenitors of sdBs are located near the TRGB with masses between 1.00 and 2.00 M_\odot and metallicity $Z = 0.02$, as shown in Figure 5. We use the method in the last section to constrain the CE efficiency parameter of 8 sdB + WD binaries in Table 1. The CE efficiency parameter β_{CE} range is relatively broad from 0.01 to 1.55 (see the top panel in Figure 6). Such results are not surprising without knowing the precise masses and evolutionary stages of the sdB progenitors. The observed WD masses alone in these sdB binaries are probably not sufficient to limit the progenitor masses of sdBs. The WD masses which pair sdB progenitors with masses between 1.00 and 2.00 M_\odot are all within the error bars except for the partially less massive progenitors for PG 1043+760 and a small region of

the more massive progenitors for PG 1136-003 (see the bottom panel in Figure 6).

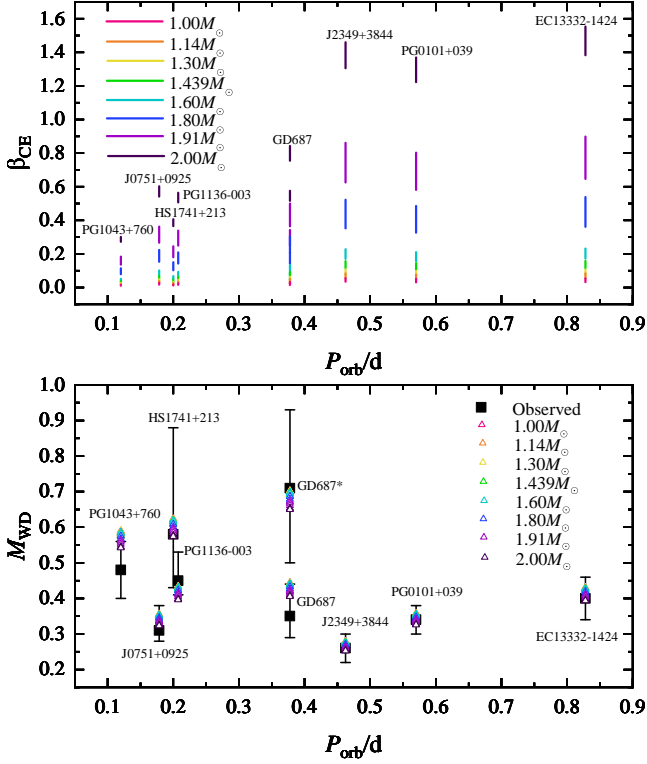


Figure 6. The CE efficiency parameter β_{CE} for sdB + WD binaries with progenitor masses between 1.00 and 2.00 M_{\odot} (top panel) and WD mass that pair the final sdB mass for the corresponding progenitor mass with the orbital period.

Aside from the WD mass M_{WD} , we further apply the $P_{\text{orb}}-M_{\text{WD}}$ relation to constrain the progenitor mass of an sdB. The progenitor mass and evolutionary stage are chosen if there is a minimum of $|P_1 - P_{\text{theo}}|/P_{\text{theo}}$ from the model grids (Figure 5). Then, we successfully identify the progenitor masses and radii of 7 systems at the onset of the CE process (see Table 2). The minima $|P_1 - P_{\text{theo}}|/P_{\text{theo}}$ for GALEXJ075147.0+092526, PG1136-003, PG0101+039, and EC13332-1424 are all less than 0.002. The minimum $|P_1 - P_{\text{theo}}|/P_{\text{theo}}$ of GD687* is 0.15. We find the $P_{\text{orb}}-M_{\text{WD}}$ relation becomes less restrictive for $M_{\text{WD}} > 0.5M_{\odot}$ or $M_{\text{WD}} < 0.27M_{\odot}$. For HSI1741+213 and GALEXJ234947.7+384440, we only determine the sdB mass and radius from the WD mass M_{WD} . The sdB masses of PG1043+760 and GD687 are below 0.29 M_{\odot} (Table 1). The core mass of TRGB stars decreases from about 0.47 to 0.39 M_{\odot} for progenitor mass from 1 to 2 M_{\odot} . So, the progenitor masses of these two objects are likely larger than 2.00 M_{\odot} .

Once the progenitor mass and evolutionary stage at the onset of the CE phase have been determined in reverse, the CE efficiency parameter β_{CE} of a sdB+WD object can be determined precisely rather than in a broad range (see Figure 7). The CE efficiency parameter β_{CE} is less than 0.1 for a relatively low mass progenitor. However, β_{CE} is larger than 0.3 for a relatively massive progenitor (see both Figure 7 and Table 2). The average β_{CE} is 0.32 for these sdB+WD objects (Figure 8). The CE efficiency parameter α_{CE} can be nonphysically larger than 3 without precisely calculated binding energy (gray circles in Figure 8). We present the linear fitting formula of the CE efficiency parameter β_{CE} as a function of the initial mass ratio $q_i = M_{\text{li}}/M_{\text{WD}}$. Figure 9 shows that the best fit is

$$\log_{10} \beta_{\text{fit}} = -2.29269 + 2.61693 \times \log_{10} q_i, \quad (23)$$

with a variance $s^2 = \sum_{i=1}^N (\log_{10} \beta_{\text{CE}} - \log_{10} \beta_{\text{fit}})^2 / N = 0.051$. A similar relation (the gray dashed line in Figure 9) of the CE efficiency parameter and the initial mass ratio was found by De Marco et al. (2011). The gray-dashed line represents their relation from the post-RGB stars or the central stars of the planetary nebula. In their work, the progenitor masses are from 1 to 5 M_{\odot} , while in this study, the mass range is from 1 to 2 M_{\odot} . This work's steeper gradient might indicate that the lower-mass RGB stars are more unbound than massive RGB stars.

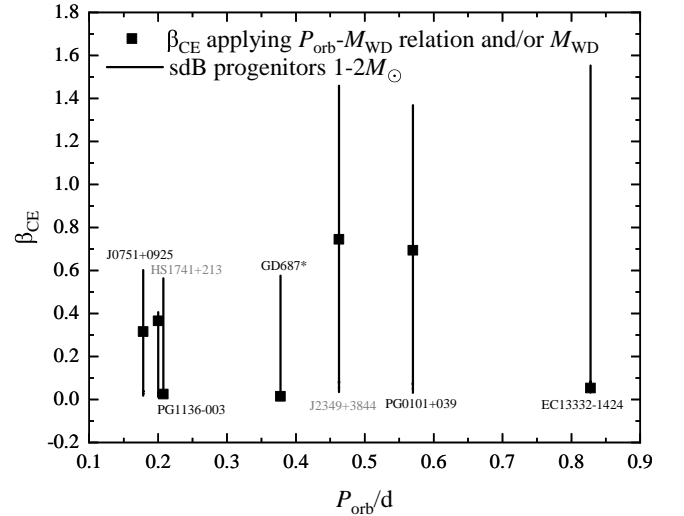


Figure 7. The CE efficiency parameter β_{CE} for 7 sdB+WD objects. The solid lines are for sdB progenitor masses from 1 (bottom) to 2 M_{\odot} (top). The filled squares are constrained by applying the $P_{\text{orb}}-M_{\text{WD}}$ relation and WD mass. Object names in gray do not follow the $P_{\text{orb}}-M_{\text{WD}}$ relation.

Table 2. Possible progenitors of sdBs

Name1	M_{1i}/M_{\odot}	R_{1i}/R_{\odot}	M_{sdB}/M_{\odot}	R_{1f}/R_{\odot}	M_{WD}/M_{\odot}	$\frac{ dP }{P}$	β_{CE}	$\log_{10}(-E_{\text{bind}}/\text{erg})$	λ	q	q_{ec}	η	γ	$\alpha_{\text{CE}}\lambda$
J0751+0925	1.91	79.498	0.410	0.479	0.333	0.001	0.316	46.814	2.073	1.230	3.661	1.695	1.230	0.661
HS1741+213	2.00	60.569	0.392	0.493	0.578	0.385	0.366	47.016	1.941	0.679	4.141	2.074	1.199	0.720
PG1136-003	1.00	151.460	0.444	0.539	0.425	0.001	0.025	45.802	2.195	1.046	1.258	5.133	1.729	0.056
GD687*	1.00	174.780	0.464	0.795	0.702	0.152	0.014	45.581	3.055	0.660	1.165	7.112	1.782	0.045
J2349+3844	1.91	79.498	0.411	0.923	0.260	0.652	0.744	46.804	2.120	1.577	3.661	1.410	1.212	1.602
PG0101+039	1.91	79.498	0.411	1.040	0.335	0.002	0.693	46.803	2.125	1.225	3.661	1.505	1.210	1.498
EC13332-1424	1.14	164.530	0.463	1.376	0.430	0.001	0.053	45.736	3.267	1.077	1.472	3.830	1.589	0.174

NOTE—1. The sdB masses of PG1043+760 and GD687 are below $0.29 M_{\odot}$. Their progenitor masses are probably larger than $2.00 M_{\odot}$.

2. The sdB masses and evolutionary stages of HS1741+213 and J2349+3844 are only constrained from the closest M_{WD} . The $P_{\text{orb}}-M_{\text{WD}}$ relation becomes less restrictive for $M_{\text{WD}} > 0.5 M_{\odot}$ or $M_{\text{WD}} < 0.27 M_{\odot}$.

3. The * marks the data of Geier et al. (2010). The minimum $|P_i - P_{\text{theo}}|/P_{\text{theo}}$ of GD687 is 0.15. For the rest, $|P_i - P_{\text{theo}}|/P_{\text{theo}}$ values is less than 0.002.

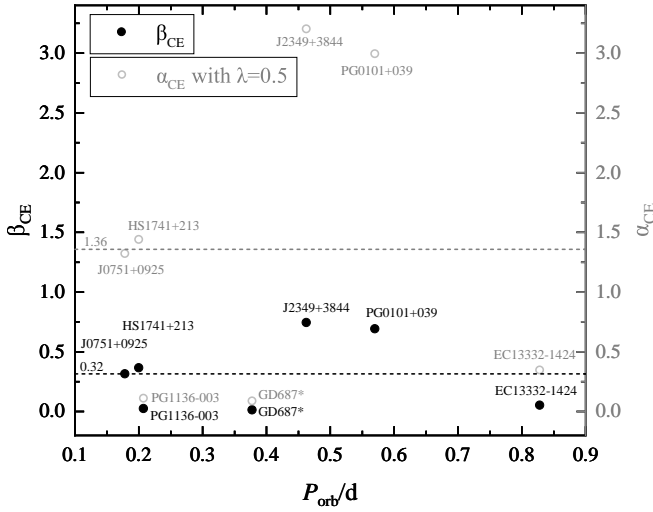


Figure 8. A comparison of CE efficiency parameters β_{CE} and α_{CE} for sdB+WD binaries. The binding energy is calculated by Equation 13 for β_{CE} (black dots) or by assuming $\lambda = 0.5$ on the right side of Equation 11 (gray circles). Black and gray dashed lines show the average β_{CE} and α_{CE} . Without realistic binding energy, the CE efficiency parameter α_{CE} might be inauthentic and greater than 1.

We systematically compare the CE efficiency parameters in different formalisms for sdB+WD binaries with determined progenitor mass and evolutionary stage. The α and β formalisms are based on an energy conservation assumption, and can be calculated from Equations 15 and 10 (or 20). Suppose we assume the structure parameter $\lambda = 0.5$ in Equation 11. The CE efficiency pa-

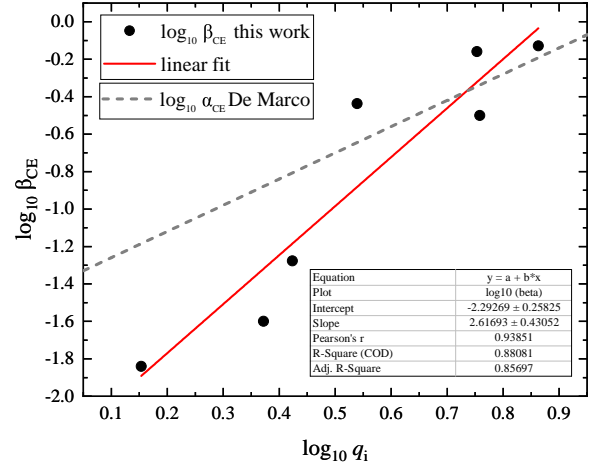


Figure 9. The linear fitting formula of the CE efficiency parameter $\log_{10} \beta_{\text{CE}}$ as a function of the initial mass ratio $\log_{10} q_i = \log_{10} M_{1i}/M_{\text{WD}}$ (red solid line). For comparison, we plot the fit of the CE efficiency parameter and initial mass ratio for post-red giant branch binaries and central stars of the planetary nebula by De Marco et al. (2011).

parameter α_{CE} can increase to over 3^1 for J2349+3844 and PG0101+039 (black open-squares in Figure 10). However, suppose we use E_{bind} from Equation 12 based on the core mass of the initial model. In that case, we find the CE efficiency parameter α_{CE} (gray open-squares) to be almost the same as β_{CE} (red squares in Figure 10). The CE efficiency parameters β_{CE} are derived from Equations 13 and 15. We fit the CE efficiency pa-

¹ The upper limit of α_{CE} in our treatment is, in principle, 1. However, some new studies claim α_{CE} as large as three or more. A more significant α_{CE} might mean that there is another energy source, such as jets (Grichener 2023), absorption of nuclear luminosity (Ivanova et al. 2001) or radiative pressure (private communication with Zhuo Chen).

parameter β_{CE} as a function of the envelope mass of the donor and the sum of the remnant mass of the donor and the WD mass as

$$\log_{10} \beta_{\text{CE}} = -1.03154 + 2.4801 \times \log_{10} \frac{M_{1e}}{M_{1f} + M_{\text{WD}}}. \quad (24)$$

The γ and η formalisms are based on angular momentum, and can be calculated from Equations 21 and 16. We plot γ and η of these sdB+WD binaries with purple and blue squares in Figure 10. We found γ is between 1.20 and 1.78. Inspired by Di Stefano et al. (2023), we fit η for seven short orbital sdB+WD binaries and find

$$\log_{10} \eta = 0.5077 - 0.99168 \times \log_{10} \frac{M_{1e}}{M_{1f} + M_{\text{WD}}}. \quad (25)$$

5. UNCERTAINTIES IN THE PROGENITOR MASS AND THE EVOLUTIONARY STAGE

Determination of the progenitor mass and the evolutionary stage becomes indispensable in understanding the detailed CE evolution. As discussed by Scherbak & Fuller (2023), the main uncertainty in the CE efficiency parameter α_{CE} arises from the uncertain progenitor mass of WD binaries. In addition, different evolutionary stages (RGB or asymptotic giant branch) of the progenitor (Zorotovic et al. 2010) should also play an important role. Recently, Zorotovic & Schreiber (2022) constrained the WD progenitor mass through the age of the simultaneously born brown dwarf companion. Similarly, the progenitor mass of an inner WD binary could be constrained if the age of a third star in a widely separated tertiary is known (Toonen et al. 2016).

We use the previously found orbital period and WD mass ($P_{\text{orb}}-M_{\text{WD}}$) relation (STFW14) to constrain the sdB progenitor mass and the evolutionary stage. The CE efficiency parameter could be determined more precisely once the sdB progenitor mass and the evolutionary stage are constrained. The sdB progenitor could have accreted mass from its companion in the first stable mass transfer process, and the progenitor mass and lifetime could be slightly changed (Scherbak & Fuller 2023). The main effect would be on the lifetime and the ratio of the core mass and the envelope mass of the sdB progenitor. Our results should be the same: the sdB progenitor remains in quasi-thermal equilibrium during the first mass transfer.

In principle, the $P_{\text{orb}}-M_{\text{WD}}$ relation can constrain the mass and evolutionary state of degenerate core progenitors that have suffered a first stable mass transfer and later undergo a CE phase. It is necessary for us to comprehend the mass range of the WD and the proper metallicity before using the relation. The STFW14 $P_{\text{orb}}-M_{\text{WD}}$ relation works fine for short orbital

sdB+WD binaries with M_{WD} from 0.27 to 0.50 M_{\odot} . In addition to sdB+WD binaries, our method to constrain the progenitors by applying the $P_{\text{orb}}-M_{\text{WD}}$ relation can be extended to other WD binaries.

6. UNCERTAINTIES IN THE BINDING ENERGY

To constrain the CE evolution outcome accurately, we need to solve for the envelope binding energy precisely. We discuss four major impacts on this binding energy. First, we find in Figure 4 of Paper I that companions with different masses can spiral into different positions of the donor. This means that the remnant of the donor may have a slightly thicker envelope mass for a more massive companion. In this case, the absolute value of binding energy is supposed to be slightly smaller than that customarily defined at the helium core. Secondly, the donor's remnant is supposed to expand after the thick envelope is ejected. Hence, the absolute value of binding energy can be slightly smaller again. However, even though the donor remnant can expand by a factor of 2, the binding energy hardly changes for donor stars with a degenerate core. Thirdly, all the contribution of the internal energy in Equation 12 is considered. The positive internal energy E_{th} plus the negative potential energy E_{grav} make the total binding energy E_{bind} less negative or even positive for relatively less massive TRGB stars (Han et al. 2012). Fourth, we build the progenitor model grids without considering stellar winds. Scherbak & Fuller (2023) argue that winds may decrease the progenitor mass by up to about 10 percent (De Marco et al. 2011) at the time of the CE evolution, but is a small effect relative to other uncertainties. Tout & Eggleton (1988) would argue for even more mass loss prior to CE evolution.

We examine the influence of the thermal efficiency α_{th} on the CE efficiency parameter β_{CE} . By assuming α_{th} decreases from 1 to 0, the contribution of the internal energy diminishes and vanishes. The binding energy E_{bind} becomes more negative and corresponds to a more significant CE efficiency parameter β_{CE} (Figure 11). Theoretically, the maximum of β_{CE} should be 1 in our treatment. However, if the companion launches jets, the CE efficiency parameter can be larger (Grichener 2023). So, for relatively more massive progenitors (1.9 or 2.0 M_{\odot}), the thermal efficiency α_{th} is suggested to be close to 1 (Figure 11). If there is a constant CE efficiency parameter, the thermal efficiency of relatively less massive progenitors is likely to be smaller.

As we discussed in Paper I, we calculate the binding energy of the donor by tracing the change of total energy as a function of its remnant mass (see Equation 13). So, the first three impacts on the binding energy are natu-

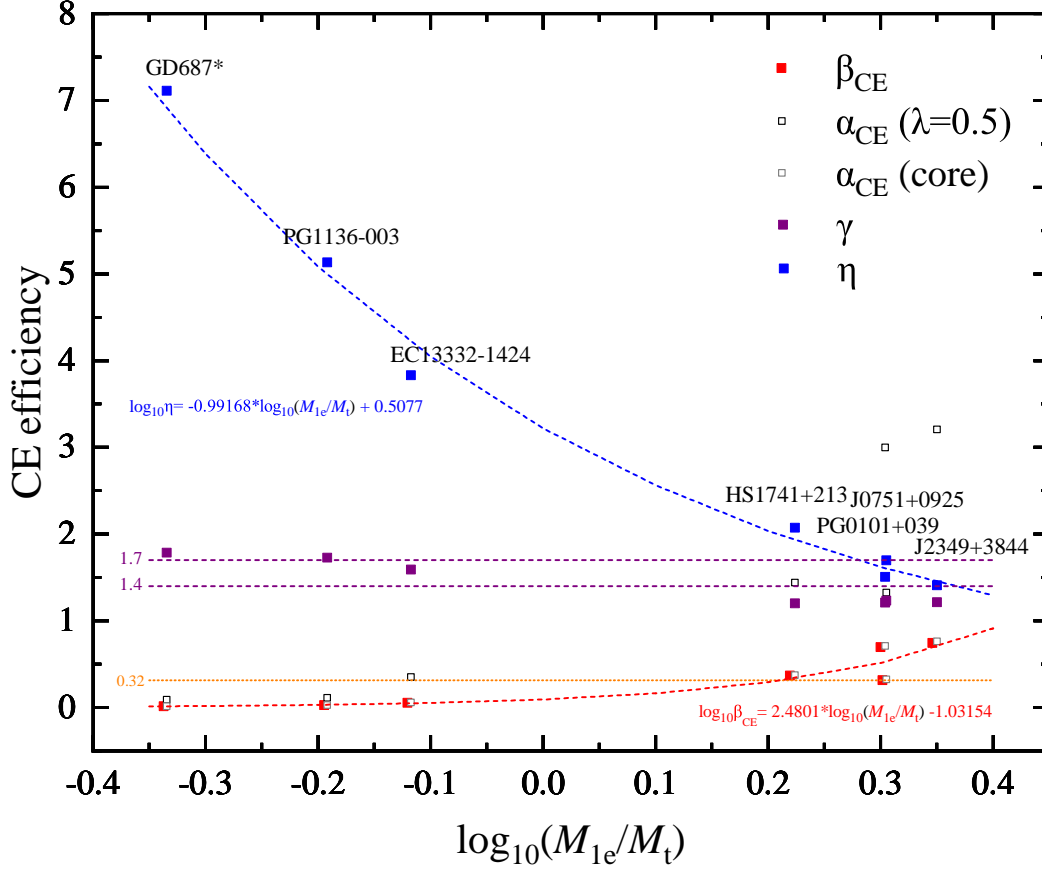


Figure 10. A systematic comparison of parameters in different CE formalisms for 7 observed sdB+WD binaries. The x-axis is defined as $M_{1e}/M_t = (M_{1i} - M_{1f})/(M_{1f} + M_2)$. Red squares present the β_{CE} values from Equation 15. Black and gray open-squares show the α_{CE} values from Equation 20 with the binding energy E_{bind} from $\lambda = 0.5$ and Equation 12. Purple squares demonstrate γ values from Equation 21. Blue squares are η values from Equation 16.

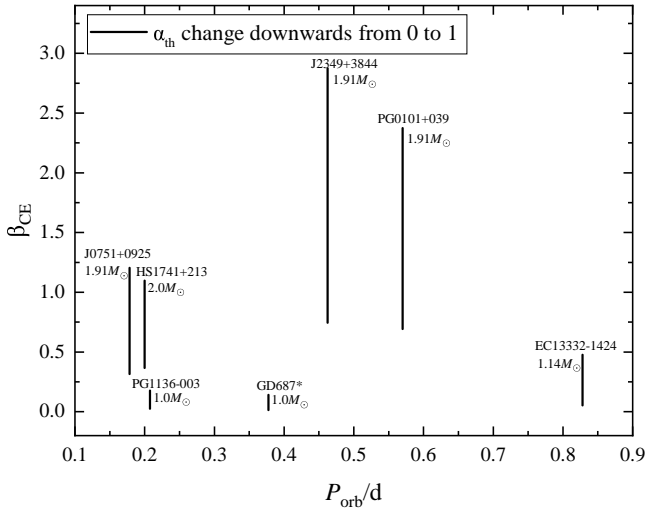


Figure 11. The impact of the internal energy on the CE efficiency parameter.

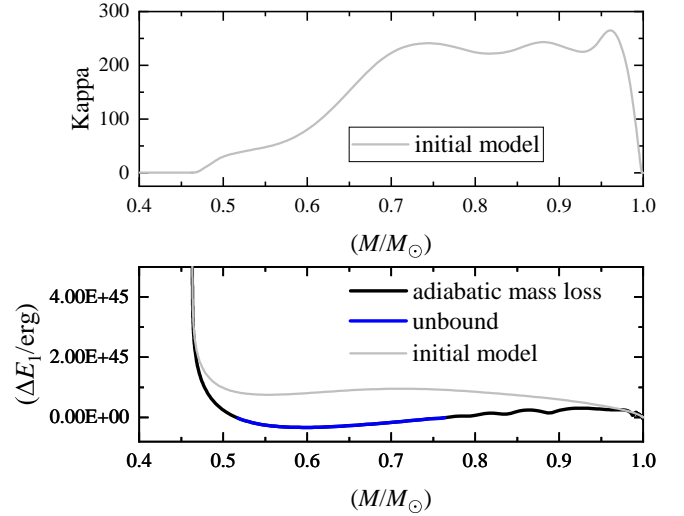


Figure 12. The opacity profile (upper panel) and different E_{bind} against the mass or remnant mass of the $1 M_{\odot}$ and $174.78 R_{\odot}$ TRGB star.

rally addressed. Compared with the initial model before CE, the envelope response becomes vital after reaching the partial ionization zones (Figure 12). For the remnant mass between 0.764 and $0.517 M_{\odot}$, the binding energy $E_{\text{bind}} = -\Delta E_1$ even becomes positive. This positive case is, at some level, similar to finding less massive TRGB donors (Han et al. 2012). However, as the remnant mass approaches the donor’s degenerate core, the binding energy difference between E_{bind} and E'_{bind} becomes smaller again. Hence, the first two impacts discussed above only need to be concerned with donors with non-degenerate cores. For these short orbital sdB+WD binaries, we find the difference between CE efficiency parameters β_{CE} and α_{CE} is relatively small (Figure 10). Future binary population synthesis simulations of sdB binaries, applying a more accurate CE efficiency from fitted formulae 23 and 24 and previously found binding energy (Tauris & Dewi 2001; Xu & Li 2010; Loveridge et al. 2011; De Marco et al. 2011) are needed.

7. COMPARISON OF CE EFFICIENCY WITH PREVIOUS STUDIES

The CEE outcome is essential to study the evolution and formation of short orbital-period compact binaries and double compact binaries. Energy or angular momentum conservation formulae can describe the CEE outcome. Webbink (2008) argues that any final energy state lower than the initial state requires the loss of angular momentum, and the converse is not necessarily true. So, Webbink (2008) concludes the energy budget more strongly constrains possible CEE outcomes.

The short orbital sdB+WD binaries offer the best examples to constrain CEE outcome because of the simplicity of sdB progenitors. Most sdB progenitors are located near the TRGB. Nevertheless, knowing the actual progenitor mass is necessary to constrain the CE efficiency parameter precisely. A short orbital-period sdB binary with a WD companion is likely formed after a first stable mass transfer phase and a second unstable CE phase. By applying a $P_{\text{orb}}-M_{\text{WD}}$ relation for the first stable mass transfer phase, we can precisely trace back the progenitor mass and evolutionary stage.

With an adequately (not just assuming $\lambda = 0.5$) calculated binding energy we determine the CE efficiency parameter of seven short orbital sdB+WD binaries with known inclination angles. Assuming a constant CE efficiency parameter β_{CE} exists its average is 0.32 (Figure 10). This average β_{CE} agrees with other findings from WD-binaries or WD+brwon-dwarf binaries (Scherbak & Fuller 2023; Zorotovic et al. 2010; Zorotovic & Schreiber 2022). However, this CE efficiency might also be a statistical effect of the broad progenitor

mass ranges in previous studies. We fit the CE efficiency parameter β_{CE} as a function of the initial and final binary masses (fitting formulae 23 and 24).

Nelemans et al. (2000) find γ between 1.4 and 1.7 for three helium WD systems based on their angular momentum description. Our findings are consistent with their results but with a slightly lower limit $1.78 > \gamma > 1.20$ (Figure 10). Di Stefano et al. (2023) study a large sample of post-CE WD+WD binaries based on their η description. The η in our study has the same trend as the results from Di Stefano et al. (2023) but with a steeper gradient of 0.992 instead of 0.780. However, the difference is only noticeable for $\log_{10}(M_{1e}/M_t) < 0.1$, where almost has no WD+WD samples in the study by Di Stefano et al. (2023).

8. SUMMARY AND CONCLUSION

The CEE is an essential and long discussed physical stage in binary star evolution. Its outcome is related to the evolution and formation of many short orbital-period compact binaries, including the progenitors of merging stellar gravitational wave sources. Short orbital-period sdB+WD binaries, formed after a first stable mass transfer phase and a second unstable CE phase, are excellent samples to study the fundamental process of the CEE. By applying a $P_{\text{orb}}-M_{\text{WD}}$ relation from the first stable mass transfer process, the progenitor mass and evolutionary stage of the current sdB can be precisely constrained. A sound $P_{\text{orb}}-M_{\text{WD}}$ relation is, in principle, suitable to constrain the CEE outcome of other WD binaries.

By assuming an adiabatic CE ejection process, we trace the donor’s total energy change as a function of its remnant mass. The response of the stellar interior to mass loss is naturally addressed. We use a total energy conservation assumption, plus the need for both components to shrink back within their Roche lobes, to constrain the CEE outcome of seven short orbital period sdB+WD binaries. The average CE efficiency parameters in this study are consistent with previous studies (Zorotovic et al. 2010; Hernandez et al. 2022; Zorotovic & Schreiber 2022; Scherbak & Fuller 2023). With well-constrained sdB progenitor masses and evolutionary stages, the CE efficiency parameter is fitted as a function of the initial mass ratio (Equation 23) and other forms (Equation 24). In addition to energy descriptions, we also discuss the results from angular momentum descriptions.

The impact of different binding energy calculations on the CE efficiency parameter is small. This result is as we expected because the envelope mass of an sdB is tiny. However, the impact would become more critical

for other post-CE binaries with more massive progenitors, especially those with none-degenerate cores. The binding energy is also sensitive to the internal energy. For relatively more massive progenitors in these seven sdB+WD binaries the thermal efficiency α_{th} needs to be close to 1.

Acknowledgments

We wish to thank the referee for his valuable comments and suggestions, which have helped us further improve this work. This project is supported by the National Natural Science Foundation of China (NSFC, grant Nos. 12288102, 12125303), National Key R&D Program of China (2021YFA1600403,

2021YFA1600401), NSFC (grant Nos. 12090040/3, 12173081), Yunnan Fundamental Research Projects (grant NOs. 202101AV070001), Yunnan Revitalization Talent Support Program - Science & Technology Champion Project (No. 202305AB350003), and International Centre of Supernovae, Yunnan Key Laboratory (No. 202302AN360001), the Key Research Program of Frontier Sciences, CAS, No. ZDBS-LY-7005, CAS, Light of West China Program and International Centre of Supernovae, Yunnan Key Laboratory (No. 202302AN360001). CAT thanks Churchill College for his fellowship. AS thanks the Gates Cambridge Trust for his scholarship.

REFERENCES

- Belczynski, K., Kalogera, V., & Bulik, T. 2002, *ApJ*, 572, 407, doi: [10.1086/340304](https://doi.org/10.1086/340304)
- Bhattacharya, D., & van den Heuvel, E. P. J. 1991, *PhR*, 203, 1, doi: [10.1016/0370-1573\(91\)90064-S](https://doi.org/10.1016/0370-1573(91)90064-S)
- Broekgaarden, F. S., Berger, E., Neijssel, C. J., et al. 2021, *MNRAS*, 508, 5028, doi: [10.1093/mnras/stab2716](https://doi.org/10.1093/mnras/stab2716)
- Cai, Y. Z., Pastorello, A., Fraser, M., et al. 2022, *A&A*, 667, A4, doi: [10.1051/0004-6361/202244393](https://doi.org/10.1051/0004-6361/202244393)
- Chen, W. C., & Liu, W. M. 2013, *MNRAS*, 432, L75, doi: [10.1093/mnrasl/slt043](https://doi.org/10.1093/mnrasl/slt043)
- Chen, X., Han, Z., Deca, J., & Podsiadlowski, P. 2013, *MNRAS*, 434, 186, doi: [10.1093/mnras/stt992](https://doi.org/10.1093/mnras/stt992)
- Copperwheat, C. M., Morales-Rueda, L., Marsh, T. R., Maxted, P. F. L., & Heber, U. 2011, *MNRAS*, 415, 1381, doi: [10.1111/j.1365-2966.2011.18786.x](https://doi.org/10.1111/j.1365-2966.2011.18786.x)
- de Kool, M. 1990, *ApJ*, 358, 189, doi: [10.1086/168974](https://doi.org/10.1086/168974)
- De Marco, O., Passy, J.-C., Moe, M., et al. 2011, *MNRAS*, 411, 2277, doi: [10.1111/j.1365-2966.2010.17891.x](https://doi.org/10.1111/j.1365-2966.2010.17891.x)
- Di Stefano, R., Kruckow, M. U., Gao, Y., Neunteufel, P. G., & Kobayashi, C. 2023, *ApJ*, 944, 87, doi: [10.3847/1538-4357/aca9b](https://doi.org/10.3847/1538-4357/aca9b)
- Eggleton, P. P. 1983, *ApJ*, 268, 368, doi: [10.1086/160960](https://doi.org/10.1086/160960)
- Gallegos-Garcia, M., Berry, C. P. L., & Kalogera, V. 2023, *ApJ*, 955, 133, doi: [10.3847/1538-4357/ace434](https://doi.org/10.3847/1538-4357/ace434)
- Gao, S.-J., & Li, X.-D. 2023, *MNRAS*, 525, 2605, doi: [10.1093/mnras/stad2446](https://doi.org/10.1093/mnras/stad2446)
- Ge, H., Hjellming, M. S., Webbink, R. F., Chen, X., & Han, Z. 2010a, *ApJ*, 717, 724, doi: [10.1088/0004-637X/717/2/724](https://doi.org/10.1088/0004-637X/717/2/724)
- Ge, H., Tout, C. A., Chen, X., et al. 2023, *ApJ*, 945, 7, doi: [10.3847/1538-4357/acb7e9](https://doi.org/10.3847/1538-4357/acb7e9)
- Ge, H., Webbink, R. F., Chen, X., & Han, Z. 2015, *ApJ*, 812, 40, doi: [10.1088/0004-637X/812/1/40](https://doi.org/10.1088/0004-637X/812/1/40)
- . 2020a, *ApJ*, 899, 132, doi: [10.3847/1538-4357/aba7b7](https://doi.org/10.3847/1538-4357/aba7b7)
- Ge, H., Webbink, R. F., & Han, Z. 2020b, *ApJS*, 249, 9, doi: [10.3847/1538-4365/ab98f6](https://doi.org/10.3847/1538-4365/ab98f6)
- Ge, H., Webbink, R. F., Han, Z., & Chen, X. 2010b, *Ap&SS*, 329, 243, doi: [10.1007/s10509-010-0286-1](https://doi.org/10.1007/s10509-010-0286-1)
- Ge, H., Tout, C. A., Chen, X., et al. 2022, *ApJ*, 933, 137, doi: [10.3847/1538-4357/ac75d3](https://doi.org/10.3847/1538-4357/ac75d3)
- Geier, S. 2020, *A&A*, 635, A193, doi: [10.1051/0004-6361/202037526](https://doi.org/10.1051/0004-6361/202037526)
- Geier, S., Heber, U., Kupfer, T., & Napiwotzki, R. 2010, *A&A*, 515, A37, doi: [10.1051/0004-6361/200912545](https://doi.org/10.1051/0004-6361/200912545)
- Geier, S., Hirsch, H., Tillich, A., et al. 2011, *A&A*, 530, A28, doi: [10.1051/0004-6361/201015316](https://doi.org/10.1051/0004-6361/201015316)
- Grichener, A. 2023, *MNRAS*, 523, 221, doi: [10.1093/mnras/stad1449](https://doi.org/10.1093/mnras/stad1449)
- Han, Z., Chen, X., Lei, Z., & Podsiadlowski, P. 2012, in *Astronomical Society of the Pacific Conference Series*, Vol. 452, Fifth Meeting on Hot Subdwarf Stars and Related Objects, ed. D. Kilkenney, C. S. Jeffery, & C. Koen, 3
- Han, Z., Podsiadlowski, P., & Eggleton, P. P. 1995, *MNRAS*, 272, 800, doi: [10.1093/mnras/272.4.800](https://doi.org/10.1093/mnras/272.4.800)
- Han, Z., Podsiadlowski, P., Maxted, P. F. L., & Marsh, T. R. 2003, *MNRAS*, 341, 669, doi: [10.1046/j.1365-8711.2003.06451.x](https://doi.org/10.1046/j.1365-8711.2003.06451.x)
- Han, Z., Podsiadlowski, P., Maxted, P. F. L., Marsh, T. R., & Ivanova, N. 2002, *MNRAS*, 336, 449, doi: [10.1046/j.1365-8711.2002.05752.x](https://doi.org/10.1046/j.1365-8711.2002.05752.x)
- Heber, U. 2009, *ARA&A*, 47, 211, doi: [10.1146/annurev-astro-082708-101836](https://doi.org/10.1146/annurev-astro-082708-101836)
- . 2016, *PASP*, 128, 082001, doi: [10.1088/1538-3873/128/966/082001](https://doi.org/10.1088/1538-3873/128/966/082001)
- Hernandez, M. S., Schreiber, M. R., Parsons, S. G., et al. 2022, *MNRAS*, 517, 2867, doi: [10.1093/mnras/stac2837](https://doi.org/10.1093/mnras/stac2837)
- Iben, I., J., & Tutukov, A. V. 1984, *ApJS*, 54, 335, doi: [10.1086/190932](https://doi.org/10.1086/190932)

- Iorio, G., Mapelli, M., Costa, G., et al. 2023, *MNRAS*, 524, 426, doi: [10.1093/mnras/stad1630](https://doi.org/10.1093/mnras/stad1630)
- Ivanova, N., Podsiadlowski, P., & Spruit, H. 2001, in *Astronomical Society of the Pacific Conference Series*, Vol. 229, *Evolution of Binary and Multiple Star Systems*, ed. P. Podsiadlowski, S. Rappaport, A. R. King, F. D’Antona, & L. Burderi, 261, doi: [10.48550/arXiv.astro-ph/0102141](https://doi.org/10.48550/arXiv.astro-ph/0102141)
- Ivanova, N., Justham, S., Chen, X., et al. 2013, *A&A Rv*, 21, 59, doi: [10.1007/s00159-013-0059-2](https://doi.org/10.1007/s00159-013-0059-2)
- Joss, P. C., Rappaport, S., & Lewis, W. 1987, *ApJ*, 319, 180, doi: [10.1086/165443](https://doi.org/10.1086/165443)
- Kashi, A., & Soker, N. 2011, *MNRAS*, 417, 1466, doi: [10.1111/j.1365-2966.2011.19361.x](https://doi.org/10.1111/j.1365-2966.2011.19361.x)
- Kawka, A., Vennes, S., O’Toole, S., et al. 2015, *MNRAS*, 450, 3514, doi: [10.1093/mnras/stv821](https://doi.org/10.1093/mnras/stv821)
- Kippenhahn, R., & Weigert, A. 1967, *ZA*, 65, 251
- Kupfer, T., Geier, S., Heber, U., et al. 2015, *A&A*, 576, A44, doi: [10.1051/0004-6361/201425213](https://doi.org/10.1051/0004-6361/201425213)
- Lei, Z., He, R., Németh, P., et al. 2023, *ApJ*, 942, 109, doi: [10.3847/1538-4357/aca542](https://doi.org/10.3847/1538-4357/aca542)
- Li, Z., Chen, X., Ge, H., Chen, H.-L., & Han, Z. 2023, *A&A*, 669, A82, doi: [10.1051/0004-6361/202243893](https://doi.org/10.1051/0004-6361/202243893)
- Liu, D., Wang, B., Chen, W., Zuo, Z., & Han, Z. 2018, *MNRAS*, 477, 384, doi: [10.1093/mnras/sty561](https://doi.org/10.1093/mnras/sty561)
- Livio, M., & Soker, N. 1988, *ApJ*, 329, 764, doi: [10.1086/166419](https://doi.org/10.1086/166419)
- Loveridge, A. J., van der Sluys, M. V., & Kalogera, V. 2011, *ApJ*, 743, 49, doi: [10.1088/0004-637X/743/1/49](https://doi.org/10.1088/0004-637X/743/1/49)
- Luo, Y., Németh, P., Wang, K., Wang, X., & Han, Z. 2021, *ApJS*, 256, 28, doi: [10.3847/1538-4365/ac11f6](https://doi.org/10.3847/1538-4365/ac11f6)
- Matsumoto, T., & Metzger, B. D. 2022, *ApJ*, 938, 5, doi: [10.3847/1538-4357/ac6269](https://doi.org/10.3847/1538-4357/ac6269)
- Maxted, P. F. L., Heber, U., Marsh, T. R., & North, R. C. 2001, *MNRAS*, 326, 1391, doi: [10.1111/j.1365-2966.2001.04714.x](https://doi.org/10.1111/j.1365-2966.2001.04714.x)
- Metzger, B. D. 2022, *ApJ*, 932, 84, doi: [10.3847/1538-4357/ac6d59](https://doi.org/10.3847/1538-4357/ac6d59)
- Nelemans, G., & Tout, C. A. 2005, *MNRAS*, 356, 753, doi: [10.1111/j.1365-2966.2004.08496.x](https://doi.org/10.1111/j.1365-2966.2004.08496.x)
- Nelemans, G., Verbunt, F., Yungelson, L. R., & Portegies Zwart, S. F. 2000, *A&A*, 360, 1011, doi: [10.48550/arXiv.astro-ph/0006216](https://doi.org/10.48550/arXiv.astro-ph/0006216)
- Olejak, A., Belczynski, K., & Ivanova, N. 2021, *A&A*, 651, A100, doi: [10.1051/0004-6361/202140520](https://doi.org/10.1051/0004-6361/202140520)
- Paczyński, B. 1971a, *AcA*, 21, 417
- . 1971b, *ARA&A*, 9, 183, doi: [10.1146/annurev.aa.09.090171.001151](https://doi.org/10.1146/annurev.aa.09.090171.001151)
- Paczynski, B. 1976, in *Structure and Evolution of Close Binary Systems*, ed. P. Eggleton, S. Mitton, & J. Whelan, Vol. 73, 75
- Podsiadlowski, P., Han, Z., Lynas-Gray, A. E., & Brown, D. 2008, in *Astronomical Society of the Pacific Conference Series*, Vol. 392, *Hot Subdwarf Stars and Related Objects*, ed. U. Heber, C. S. Jeffery, & R. Napiwotzki, 15, doi: [10.48550/arXiv.0808.0574](https://doi.org/10.48550/arXiv.0808.0574)
- Podsiadlowski, P., & Rappaport, S. 2000, *ApJ*, 529, 946, doi: [10.1086/308323](https://doi.org/10.1086/308323)
- Politano, M., Taam, R. E., van der Sluys, M., & Willems, B. 2008, *ApJL*, 687, L99, doi: [10.1086/593328](https://doi.org/10.1086/593328)
- Pols, O. R., Tout, C. A., Eggleton, P. P., & Han, Z. 1995, *MNRAS*, 274, 964, doi: [10.1093/mnras/274.3.964](https://doi.org/10.1093/mnras/274.3.964)
- Rappaport, S., Podsiadlowski, P., Joss, P. C., Di Stefano, R., & Han, Z. 1995, *MNRAS*, 273, 731, doi: [10.1093/mnras/273.3.731](https://doi.org/10.1093/mnras/273.3.731)
- Refsdal, S., & Weigert, A. 1971, *A&A*, 13, 367
- Röpke, F. K., & De Marco, O. 2023, *Living Reviews in Computational Astrophysics*, 9, 2, doi: [10.1007/s41115-023-00017-x](https://doi.org/10.1007/s41115-023-00017-x)
- Saio, H., & Jeffery, C. S. 2000, *MNRAS*, 313, 671, doi: [10.1046/j.1365-8711.2000.03221.x](https://doi.org/10.1046/j.1365-8711.2000.03221.x)
- Schaffenroth, V., Barlow, B. N., Pelisoli, I., Geier, S., & Kupfer, T. 2023, *A&A*, 673, A90, doi: [10.1051/0004-6361/202244697](https://doi.org/10.1051/0004-6361/202244697)
- Schaffenroth, V., Pelisoli, I., Barlow, B. N., Geier, S., & Kupfer, T. 2022, *A&A*, 666, A182, doi: [10.1051/0004-6361/202244214](https://doi.org/10.1051/0004-6361/202244214)
- Scherbak, P., & Fuller, J. 2023, *MNRAS*, 518, 3966, doi: [10.1093/mnras/stac3313](https://doi.org/10.1093/mnras/stac3313)
- Shao, Y., & Li, X.-D. 2021, *ApJ*, 920, 81, doi: [10.3847/1538-4357/ac173e](https://doi.org/10.3847/1538-4357/ac173e)
- Smedley, S. L., Tout, C. A., Ferrario, L., & Wickramasinghe, D. T. 2014, *MNRAS*, 437, 2217, doi: [10.1093/mnras/stt2030](https://doi.org/10.1093/mnras/stt2030)
- Soker, N. 1998, *AJ*, 116, 1308, doi: [10.1086/300503](https://doi.org/10.1086/300503)
- . 2017, *MNRAS*, 470, L102, doi: [10.1093/mnrasl/slx089](https://doi.org/10.1093/mnrasl/slx089)
- Taam, R. E., & Sandquist, E. L. 2000, *ARA&A*, 38, 113, doi: [10.1146/annurev.astro.38.1.113](https://doi.org/10.1146/annurev.astro.38.1.113)
- Tauris, T. M., & Dewi, J. D. M. 2001, *A&A*, 369, 170, doi: [10.1051/0004-6361:20010099](https://doi.org/10.1051/0004-6361:20010099)
- Tauris, T. M., & Savonije, G. J. 1999, *A&A*, 350, 928, doi: [10.48550/arXiv.astro-ph/9909147](https://doi.org/10.48550/arXiv.astro-ph/9909147)
- Tauris, T. M., & van den Heuvel, E. P. J. 2023, *Physics of Binary Star Evolution. From Stars to X-ray Binaries and Gravitational Wave Sources*, doi: [10.48550/arXiv.2305.09388](https://doi.org/10.48550/arXiv.2305.09388)
- Tauris, T. M., van den Heuvel, E. P. J., & Savonije, G. J. 2000, *ApJL*, 530, L93, doi: [10.1086/312496](https://doi.org/10.1086/312496)

- Toonen, S., Hamers, A., & Portegies Zwart, S. 2016, *Computational Astrophysics and Cosmology*, 3, 6, doi: [10.1186/s40668-016-0019-0](https://doi.org/10.1186/s40668-016-0019-0)
- Tout, C. A., & Eggleton, P. P. 1988, *MNRAS*, 231, 823, doi: [10.1093/mnras/231.4.823](https://doi.org/10.1093/mnras/231.4.823)
- Vos, J., Németh, P., Vučković, M., Østensen, R., & Parsons, S. 2018, *MNRAS*, 473, 693, doi: [10.1093/mnras/stx2198](https://doi.org/10.1093/mnras/stx2198)
- Wang, B. 2018, *Research in Astronomy and Astrophysics*, 18, 049, doi: [10.1088/1674-4527/18/5/49](https://doi.org/10.1088/1674-4527/18/5/49)
- Webbink, R. F. 1984, *ApJ*, 277, 355, doi: [10.1086/161701](https://doi.org/10.1086/161701)
- Webbink, R. F. 2008, in *Astrophysics and Space Science Library*, Vol. 352, *Astrophysics and Space Science Library*, ed. E. F. Milone, D. A. Leahy, & D. W. Hobill, 233, doi: [10.1007/978-1-4020-6544-6_13](https://doi.org/10.1007/978-1-4020-6544-6_13)
- Webbink, R. F., Rappaport, S., & Savonije, G. J. 1983, *ApJ*, 270, 678, doi: [10.1086/161159](https://doi.org/10.1086/161159)
- Xu, X.-J., & Li, X.-D. 2010, *ApJ*, 716, 114, doi: [10.1088/0004-637X/716/1/114](https://doi.org/10.1088/0004-637X/716/1/114)
- Zhang, X., & Jeffery, C. S. 2012, *MNRAS*, 419, 452, doi: [10.1111/j.1365-2966.2011.19711.x](https://doi.org/10.1111/j.1365-2966.2011.19711.x)
- Zhang, Y., Chen, H., Chen, X., & Han, Z. 2021a, *MNRAS*, 502, 383, doi: [10.1093/mnras/stab020](https://doi.org/10.1093/mnras/stab020)
- Zhang, Y., Chen, H.-L., Xiong, H., Chen, X., & Han, Z. 2021b, *MNRAS*, 505, 3514, doi: [10.1093/mnras/stab1627](https://doi.org/10.1093/mnras/stab1627)
- Zorotovic, M., & Schreiber, M. 2022, *MNRAS*, 513, 3587, doi: [10.1093/mnras/stac1137](https://doi.org/10.1093/mnras/stac1137)
- Zorotovic, M., Schreiber, M. R., Gänsicke, B. T., & Nebot Gómez-Morán, A. 2010, *A&A*, 520, A86, doi: [10.1051/0004-6361/200913658](https://doi.org/10.1051/0004-6361/200913658)